



# Enhancing integrated optical circuits: optimizing all-optical NAND and NOR gates through deep learning and machine learning

Pouya Karami<sup>1</sup> · Alireza Mohamadi<sup>2</sup> · Fariborz Parandin<sup>1</sup>

Received: 21 July 2024 / Accepted: 10 December 2024

© The Author(s), under exclusive licence to Springer Science+Business Media, LLC, part of Springer Nature 2024

## Abstract

This paper proposes a two-dimensional photonic crystal structure for designing optical NAND and NOR logic gates using dielectric rods in an air substrate. The simplicity and compact size of the proposed structure make it suitable for the fabrication of integrated optical circuits. This study leverages machine learning methods, specifically the AdaBoost Regressor and Feedforward Neural Network (FNN) models, to enhance gate performance by identifying optimal parameters. Notably, this research introduces the optimization of the phase parameter and rod radius to improve gate efficiency. Additionally, we evaluated 30 different architectures to determine the best FNN model for each scenario. The proposed gates exhibit high output power for the logical “1” state and low output power for the logical “0” state, which is crucial for minimizing detection errors. Our results indicate that machine learning techniques can significantly enhance the performance and reliability of optical logic gates, paving the way for advancements in integrated optical circuit design.

**Keywords** Optical logic gates · Deep learning · Machine learning · Photonic crystal · Feedforward neural network

## 1 Introduction

The most significant invention of the past two centuries is the transistor, which has immensely impacted technological advancement. With the continuous progress in technology and the increasing demand for faster and smaller processors, reducing the size of transistors becomes more pressing. However, further size reduction leads to numerous challenges, such as heat dissipation and quantum phenomena, necessitating a search for alternatives to transistors (Roshani et al. 2022; Wei et al. 2024; Lotfi et al. 2020).

---

✉ Fariborz Parandin  
fa.parandin@iau.ac.ir

<sup>1</sup> Department of Electrical Engineering, Kermanshah Branch, Islamic Azad University, Kermanshah, Iran

<sup>2</sup> Department of Computer Engineering, Kermanshah Branch, Islamic Azad University, Kermanshah, Iran

Optical devices have emerged as a more suitable option among the proposed alternatives. Photonic crystals are periodic structures of two or more materials with different refractive indices. These structures can facilitate the propagation and control of light along specified paths. The advantages of photonic crystals include controlling light in desired pathways and miniaturizing optical circuits (Parandin et al. 2022; Gupta and Medhekar 2016; Wang et al. 2015; Parandin and Bagheri 2023; Moradi 2019; Askarian and Parandin 2023; Ghadrdan and Mansouri-Birjandi 2013; Karkhanehchi et al. 2017).

Photonic crystals possess unique optical properties that make them suitable for designing optical sensors, filters, and lasers. In the digital domain, these structures can be used in various logic gates, such as universal gates (NAND & NOR) and logical circuits like adders and decoders (Mamnoon-Sofiani and Javahernia 2023; Rani et al. 2015; Swarnakar et al. 2018; Parandin et al. 2024a, b, 2023a; Neisy et al. 2018; Mukherjee et al. 2014). Universal gates can implement any logic circuit, thus playing a crucial role in digital design. NAND and NOR gates are recognized as universal gates.

In digital electronics, logic gates form the fundamental building blocks of circuits, performing basic logical operations on binary inputs. Universal logic gates, such as NAND and NOR, are particularly important because they can be used to construct any other logic function. The NAND gate is complementary to the AND gate, and the output of this gate is set to logical “1” when at least one of the inputs is zero. NOR gate is complementary to the OR gate. The output of the NOR gate is set to “1” when both inputs are zero.

Photonic crystals are classified into one-dimensional, two-dimensional, and three-dimensional categories based on their periodicity. If the structure is periodic in one dimension, it is termed a one-dimensional photonic crystal; if in two dimensions, it is two-dimensional; and in three dimensions, it is three-dimensional (Gupta and Medhekar 2016; Swarnakar et al. 2019; Askarian 2021; Parandin and Sheykhan 2022).

A key characteristic of photonic crystals is light reflection, which occurs due to the periodic nature of the structure. This light reflection happens in all three directions for three-dimensional photonic crystal structures, making them more suitable for optical device applications. However, due to manufacturing complexities, two-dimensional structures are often preferred for designing optical circuits (Saghaei 2017; Olyaei et al. 2018; Seraj et al. 2020; Olyaei 2019).

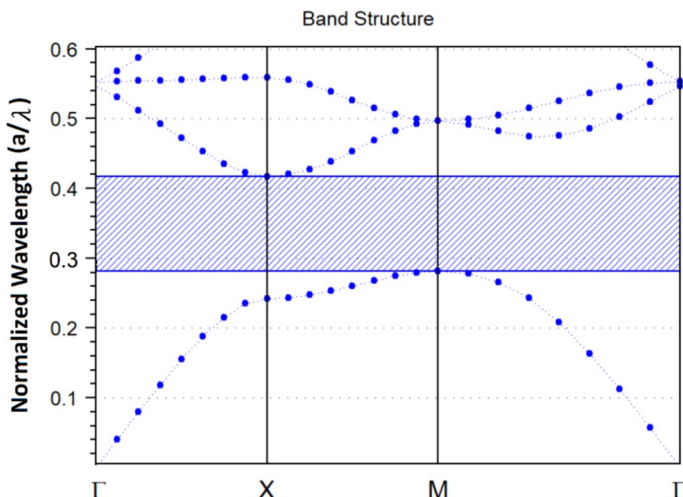
The most important features to consider when designing logic gates with photonic crystals are the small size and simplicity of the structure. These two parameters are essential for achieving high-speed integrated optical circuits and have been prioritized in the proposed structure (Parandin and Malmir 2020; Parandin 2021; Liu et al. 2013). The proposed structure is designed to function as both a NAND gate and a NOR gate by changing the phase of the inputs.

One crucial aspect in designing optical NAND and NOR gates is ensuring high optical power for the logical “1” state and low power for the logical “0” state. The significant difference between the high and low logical states is essential for minimizing detection errors at the output. Previous research emphasized applying machine learning techniques, primarily using data generated from simulations involving AND, XOR, and NOT gates (Parandin and Mohamadi 2024; Parandin and Mohammadi 2024; Mohammadi et al. 2024).

In this paper, we aim to optimize the phi parameter (phase of the input light source) and rod radius using the AdaBoost Regressor and Feedforward Neural Network (FNN) models to enhance the performance of NAND and NOR gates. Our current goal is to improve these gates’ performance by utilizing these models to identify the optimal parameters.

**Table 1** Parameters of the proposed photonic crystal structure

Parameters	Symbol	Value
Lattice constant	a	0.6 $\mu\text{m}$
Radius of rods	R	0.12 $\mu\text{m}$
Background Refractive index	$n_1$	1
Rods refractive index	$n_2$	3.46
Number of rods	—	15 $\times$ 21

**Fig. 1** Band structure for the basic photonic crystal structure

## 2 Proposed structure for creating optical NAND and NOR gates

A structure with a square lattice is employed to create universal NAND and NOR gates. Initially, a photonic crystal lattice is selected, and after calculating the band structure, the operating wavelength is determined. Waveguides are then created by introducing defects in the lattice. The physical characteristics of the initial structure are shown in Table 1.

The created structure has a photonic bandgap for TM modes, which no wavelengths can enter. This wavelength range is determined through band structure calculations. The band structure calculations indicate that this range is  $1.42\mu\text{m}$  to  $2.1\mu\text{m}$ , meaning the structure reflects all wavelengths within this range. Therefore, the input light sources can be chosen within this range. The current optical communication wavelength is  $1.55\mu\text{m}$ , so the input light sources are set to this wavelength. The Plane Wave Expansion (PWE) method is used for band structure calculations. Figure 1 shows the band structure for the basic structure of the photonic crystal.

In the proposed structure, waveguides are created for the gate inputs by removing some rods. These inputs are labeled as Input Bias, Input A, and Input B in Fig. 2. For the NAND gate, ports A and B are considered gate inputs. The bias input supplies output power when inputs A and B are off. For better results, Input A and B are set at -45

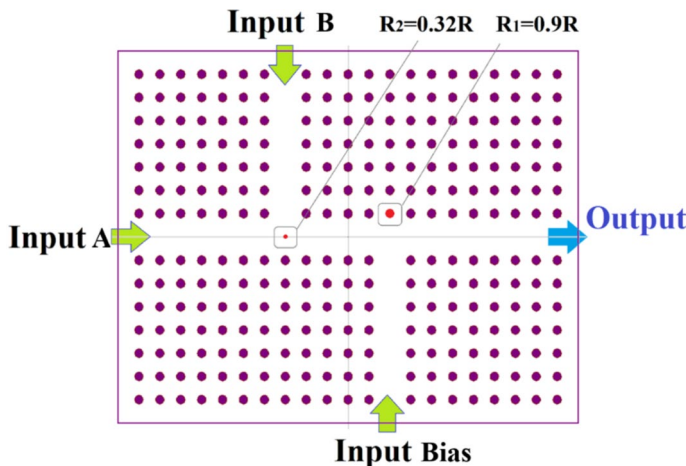


**Fig. 2** Waveguide Paths for Implementing Optical NAND and NOR Gates

and +45 degrees relative to the Bias input, respectively. These values are based on the path differences of these two inputs until they intersect with the bias input, ensuring optimal output conditions.

To achieve a NOR gate with the same structure, the phase difference for inputs A and B is set to “0” and +10 degrees, respectively. Thus, the same structure can be used for both gates, with only the input phase difference needing adjustment to switch between the gates.

In the next step, for using a single structure as universal optical NAND and NOR gates and optimizing output parameters, rods  $R_1$  and  $R_2$  are considered defect rods, and their variation determines the outputs. In this study, the AdaBoost Regressor and FNN models are harnessed to pinpoint the optimal parameters. Figure 2 illustrates the waveguide paths for the proposed design.

Based on the results, the optimal points for achieving the best output for the defect rods are  $R_1=0.9R$  and  $R_2=0.32R$ , with simulations performed accordingly. Calculations were conducted to determine the normalized output power and the power distribution along the output paths.

### 3 Methodology

In this section, we detail the methodologies employed to optimize the performance of optical gates, focusing on the precise tuning of key parameters such as rod radius and phi, which are essential for signal transmission efficiency. Advanced machine learning techniques, particularly FNNs, and the AdaBoost algorithm were applied to achieve optimal configurations. These models were instrumental in predicting the best-performing parameters by analyzing multiple input scenarios. Through an iterative process of parameter refinement and model evaluation, we aimed to enhance the efficiency of optical gates in various applications, emphasizing the reliability and accuracy of the chosen algorithms.

### 3.1 The evolution of AI and ML: from human thinking to autonomous systems

Artificial intelligence (AI) enables computers and other computer-based systems to mimic human thinking and behavior. AI research delves into understanding how the human brain processes information, learns, makes decisions, and solves problems. The goal of this expansive field is to develop intelligent machines. Machine learning (ML), a subset of AI, focuses on identifying and learning from patterns in data sets. By definition, ML is an AI application that allows systems to automatically learn and improve from experience without explicit programming (Strong 2016). Common algorithms in ML include neural networks, support vector machines, decision trees, AdaBoost algorithm, and logistic regression, among others (Geron 2019).

### 3.2 Optimizing optical gate performance: machine learning and deep learning approaches for rod radius and phi parameter tuning

Rod radios and phi are pivotal for enhancing the efficacy of optical gates, especially concerning signal transmission and processing. With their cylindrical structure and distinctive material properties, rod radios streamline the conversion of electrical signals to optical ones, ensuring minimal signal loss and maximal transmission speed. Meanwhile, phi, representing the phase disparity between input and output signals, governs crucial operational traits of the gate, including switching speed and fidelity. Fine-tuning parameters like rod radius and phi is essential for crafting high-performance optical gates, indispensable components in various optical communication and computing systems, promising expedited data processing and augmented information transmission. To achieve this optimization, we employ advanced methodologies. Specifically, the FNN model is harnessed to refine phi, while the Adaboost Regressor model is utilized to optimize the rod radius.

### 3.3 AdaBoost algorithm

AdaBoost, formally called Adaptive Boosting, stands out as a powerful machine-learning technique pioneered by Freund and Schapire. It operates by iteratively training a sequence of weak classifiers, each aimed at rectifying the errors of its predecessors. Through a clever combination of these weak learners, AdaBoost produces a final prediction model that surpasses the capabilities of any individual classifier. Its adaptability and versatility have rendered it indispensable across various domains, including classification, regression, and feature selection. AdaBoost exhibits resilience to noisy data and outliers, maintaining high predictive accuracy even in challenging environments. Furthermore, its ability to converge in accuracy, coupled with implicit regularization mechanisms, enables effective generalization and mitigates overfitting concerns. AdaBoost emerges as a robust and versatile algorithm, offering reliable performance and effective solutions to diverse machine-learning tasks (Schapire 2013).

### 3.4 Performance metrics

To identify the most accurate optical gate simulation software, we evaluated algorithms using two key metrics: Root Mean Squared Error (RMSE) and Mean Absolute Error (MAE). These metrics provide a robust assessment of model precision.

- Root Mean Squared Error (RMSE):

$$RMSE = \sqrt{\frac{\sum_{i=1}^n (Y_i - \hat{Y}_i)^2}{n}} \quad (1)$$

RMSE measures the square root of the average squared differences between the predicted values ( $\hat{Y}$ ) and the actual values ( $Y_i$ ), with  $n$  representing the number of data points. It emphasizes larger errors, offering a detailed picture of model performance.

- Mean Absolute Error (MAE):

$$MAE = \frac{\sum_{i=1}^n |Y_i - \hat{Y}_i|}{n} \quad (2)$$

MAE calculates the average absolute differences between the predicted values ( $\hat{Y}$ ) and the actual values ( $Y_i$ ). This metric, with  $n$  representing the number of data points, provides a straightforward measure of predictive accuracy by averaging the magnitude of all errors (Pedregosa et al. 2011).

### 3.5 Machine learning optimization of rod radius for enhanced performance in optical NAND gate design

The dataset used for this analysis was derived from simulations of an optical NAND gate containing various input scenarios ( $A=B=0$ ,  $A=0 B=1$ ,  $A=1 B=0$ ,  $A=B=1$ ) and corresponding output power levels. The input features were standardized to ensure uniformity and improve model performance.

Separate AdaBoost regression models were trained for each input scenario to capture the relationship between rod radius and output power accurately. This approach allowed us to address each scenario's specific characteristics and enhance the models' predictive accuracy.

Using the trained models, we generated predictions for a set of standardized random input values. These predictions were then utilized to calculate the optimal rod radius (*optimize\_R\_NAND*) using an optimization formula that balanced the predicted outputs across different scenarios. This formula is represented as:

$$\text{optimize\_R\_NAND} = \frac{(preds\_A\_1B\_0 \times preds\_A\_0B\_1 \times preds\_AB\_0)}{preds\_AB\_1} \quad (3)$$

was designed to maximize the gate's efficiency by integrating the various predicted power levels.

We introduced this formula for the first time and it can be applied to optimize any logic gate. The reason we placed *preds\_AB\_1* in the denominator is that, for a NAND gate, the

output should be zero when both inputs are one. However, for the NOR gate, we used the formula:

$$\text{optimize\_R\_NOR} = \frac{(\text{preds\_AB\_0})}{\text{preds\_A\_1B\_0} \times \text{preds\_A\_0B\_1} \times \text{preds\_AB\_1}} \quad (4)$$

In summary, we place scenarios that should be near zero in the denominator because any number with a negative exponent in the denominator becomes larger when it moves to the numerator. The smaller this number is, the greater its impact when it is moved to the numerator. This criterion allows us to identify better inputs; the larger the final value of this fraction, the more optimal the input configuration. This approach ensures we maximize the efficiency of the optical NOR gate, which can be adapted for use with any logic gate.

The performance of the AdaBoost models was evaluated by calculating the MAE for each input scenario. Low MAE values confirmed the accuracy and reliability of the models in predicting the rod radius. The optimized rod radius values derived from the model predictions significantly enhanced the performance of the optical NAND gate. The normalized power outputs and the optimized radius values were analyzed, demonstrating the reliability and effectiveness of the gate design.

Table 2 presents the MAE  $\pm$  standard deviation, calculated over 5 trials, for the AdaBoost regression models in predicting the rod radius ( $R_1$  and  $R_2$ ) for different optical NAND gate input scenarios. The results are shown for four input conditions:  $A=B=0$ ,  $A=1, B=0$ ,  $A=0, B=1$ , and  $A=B=1$ .

### 3.5.1 Step 1: selection of rod radius parameters

We employed a two-step selection process to identify the optimal rod radius parameters for our optical NAND gate design. In the first step, we utilized a trained AdaBoost model to generate predictions based on a set of standardized random input values. These predictions were then used to calculate the "*optimize\_R\_NAND*" values, which we ranked in descending order to prioritize high-performing configurations. To ensure both superior performance and minimal AdaBoost predictions (referred to as *AdaBoost\_preds\_AB\_1*), we conducted a second sorting step. Among the top candidates for "*optimize\_R\_NAND*," we selected the rod radius parameters corresponding to the lowest *AdaBoost\_preds\_AB\_1* value.

### 3.5.2 Step 2: minimum *AdaBoost\_preds\_AB\_1*

For both rod radius parameters ( $R_1$  and  $R_2$ ), we selected points with the minimum value of *AdaBoost\_preds\_AB\_1* among unique *random\_nums*. The *random\_num* represents a randomly generated number used in our model predictions to simulate different potential

**Table 2** MAE  $\pm$  Standard Deviation for AdaBoost Models in Predicting Rod Radius ( $R_1$  and  $R_2$ )

Scenario	R1 MAE (mean $\pm$ std)	R2 MAE (mean $\pm$ std)
$A=B=0$	$0.05622 \pm 0.00327$	$0.05359 \pm 0.00242$
$A=1, B=0$	$0.06710 \pm 0.00325$	$0.05486 \pm 0.00569$
$A=0, B=1$	$0.02607 \pm 0.00109$	$0.09018 \pm 0.00902$
$A=B=1$	$0.04623 \pm 0.00567$	$0.08388 \pm 0.00519$

**Table 3** Selected Rod Radius Parameters and Their output power

Scenario	R <sub>1</sub> (random num = 0.9R)	R <sub>2</sub> (random num = 0.32R)
AdaBoost_preds_AB_0	0.71	0.79
AdaBoost_preds_A_1B_0	0.54	0.64
AdaBoost_preds_A_0B_1	0.69	0.81
AdaBoost_preds_AB_1	0.06	0.15

configurations of the rod radius parameters. By minimizing *AdaBoost\_preds\_AB\_1*, we ensure the optimal performance of the NAND gate, which outputs a logical “0” only when both inputs are logical “1”. This is crucial because the correct operation of a NAND gate is essential for accurate logical computations. Table 3 summarizes the selected rod radius parameters and their corresponding output power:

- **AdaBoost\_preds\_AB\_1:** Predictions for the scenario where both inputs A and B are logical “1”.
- **AdaBoost\_preds\_A\_0B\_1:** Predictions for the scenario where input A is logical “0” and input B is logical 1.
- **AdaBoost\_preds\_A\_1B\_0:** Predictions for the scenario where input A is logical “1” and input B is logical “0”.
- **AdaBoost\_preds\_AB\_0:** Predictions for the scenario where both inputs A and B are logical “0”.

### 3.6 Exploring the foundations and variants of neural networks in deep learning

The neural networks are a family of deep learning (DL) and ML methods based on artificial neural networks (ANNs) with multi-hiding layers. Neural networks are applied in many different implementations with slight variations in their structures, such as recurrent neural networks (RNN), Artificial neural networks (ANN), and convolutional neural networks (CNN). FNNs are a foundational type of artificial neural network where information flows unidirectionally from input to output layers through one or more hidden layers. Each neuron in these layers applies a weighted sum and a non-linear activation function to its inputs, passing the result to the next layer. The primary training method for FNNs is the backpropagation algorithm, which adjusts connection weights to minimize the loss function by propagating errors backward from the output layer. FNNs have been instrumental in numerous applications, including image recognition and financial forecasting, and have been significantly enhanced by deep learning techniques (Rosenblatt 1958; Rumelhart et al. 1986; Ojha et al. 2017).

### 3.7 Optimizing neural network architectures for predicting phi 2 and phi 3 in NOR gates

In our pursuit of enhancing predictive accuracy, we meticulously explored neural network architectures tailored to optimize the predictive performance of features phi 2 and phi 3.

This endeavor aimed to elucidate optimal structures across multiple scenarios, delineated by target variables  $A=B=0$ ,  $A=0\ B=1$ ,  $A=1\ B=0$ , and  $A=B=1$ .

### 3.7.1 Base model for optimizing phi 2 and phi 3

To achieve our optimization goals, we designed a foundational neural network model that served as the basis for our experiments. This base model is a FNN constructed using the TensorFlow and Keras libraries. The architecture of the model includes:

- **Input layer:** A single input node corresponding to the feature phi 2 and phi 3 (1 neuron).
- **Hidden layers:** Two hidden layers with varying numbers of neurons to explore different architectural configurations.
- **Output layer:** Four output nodes corresponding to the target variables  $A=B=0$ ,  $A=0\ B=1$ ,  $A=1\ B=0$ , and  $A=B=1$  (4 neurons).

The hidden layers utilize the Rectified Linear Unit (ReLU) activation function, which helps mitigate the vanishing gradient problem and allows the model to capture complex patterns in the data. The output layer is a linear layer that predicts the continuous values of the target variables. The model is compiled using the Mean Squared Error (MSE) loss function and the Adam optimizer, known for efficiently handling large datasets and adaptability during training (Agarap 2018; Abadi et al. 2016).

### 3.7.2 Experimental setup

Our investigation unfolded through systematically examining various neural network configurations, encompassing diverse combinations of neurons in two hidden layers and training epochs. Each architectural permutation was meticulously crafted to leverage the predictive potential of phi 2 and phi 3 while accommodating the intricacies of the target variables.

### 3.7.3 FNN training and implementation

To predict the phase parameters phi 2 and phi 3, we employed an FNN architecture, which allowed for accurate modeling of the relationships between input parameters and the respective phi values. The model was trained using a dataset of 53 instances for each prediction, providing a sufficiently robust dataset for reliable training and inference.

The training was performed on a system with the following specifications:

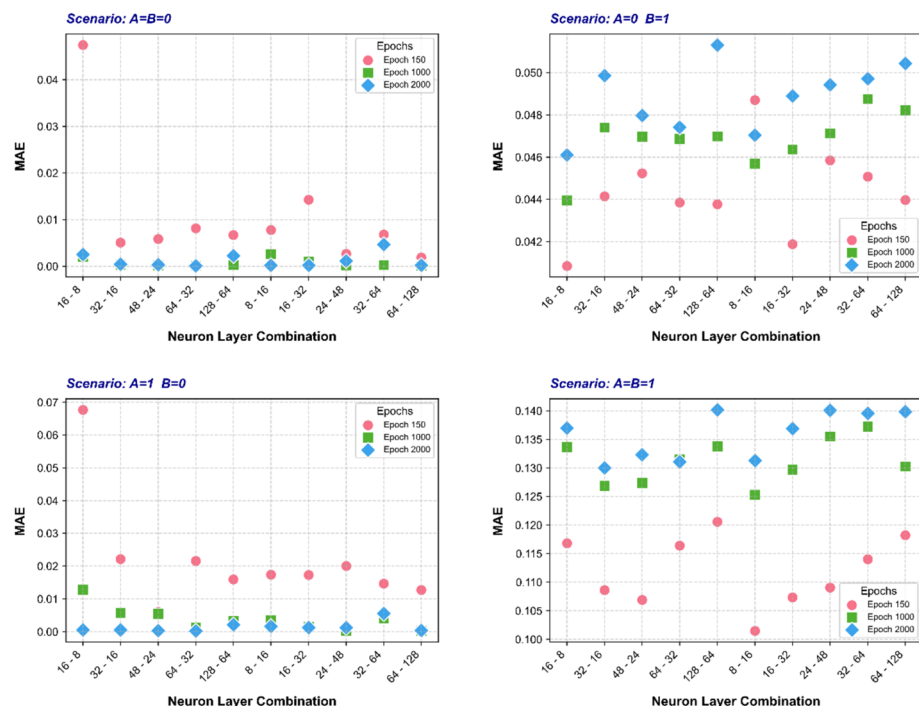
- **Processor:** Intel(R) Core(TM) i7-1065G7 CPU @ 1.30GHz, 1.50 GHz
- **RAM:** 16.0 GB

The total training time for the FNN model was approximately under 30 s. This optimization method does not require a high-performance system, as efficient computation was achieved within the given system constraints.

The reported computation times represent the total execution time for running all four scenarios with the corresponding optimal epoch values as listed in Table 4.

**Table 4** Summary of Best FNN Architectures for Predicting Phi 2 and Phi 3

Scenario	Phi 2			Phi 3		
	Neurons layer 1	Neurons layer 2	Epochs	Neurons layer 1	Neurons layer 2	Epochs
A=B=0	64	32	2000	16	8	2000
A=1, B=0	64	128	1000	8	16	150
A=0, B=1	16	8	150	16	8	150
A=B=1	8	16	150	16	8	150

**Fig. 3** Performance of FNN Models in Predicting Optimal phi 2 for NOR Gate Operation Across Different Input Scenarios

### 3.7.4 Performance of FNN models in predicting optimal phi 2 and phi 3

Figure 3 compares the MAE of 30 different FNN architectures in predicting the optimal phi parameter for an optical NOR gate. Each point represents an individual FNN architecture, with its position on the x-axis indicating the neuron layer combination (e.g., '64—32' represents an FNN with 64 neurons in the first hidden layer and 32 neurons in the second hidden layer). Different marker shapes denote the number of epochs used for training (circle: 150, square: 1000, diamond: 2000). The plots are separated based on four distinct input scenarios for the NOR gate:  $A=B=0$ ,  $A=1 B=0$ ,  $A=0 B=1$ , and  $A=B=1$ .

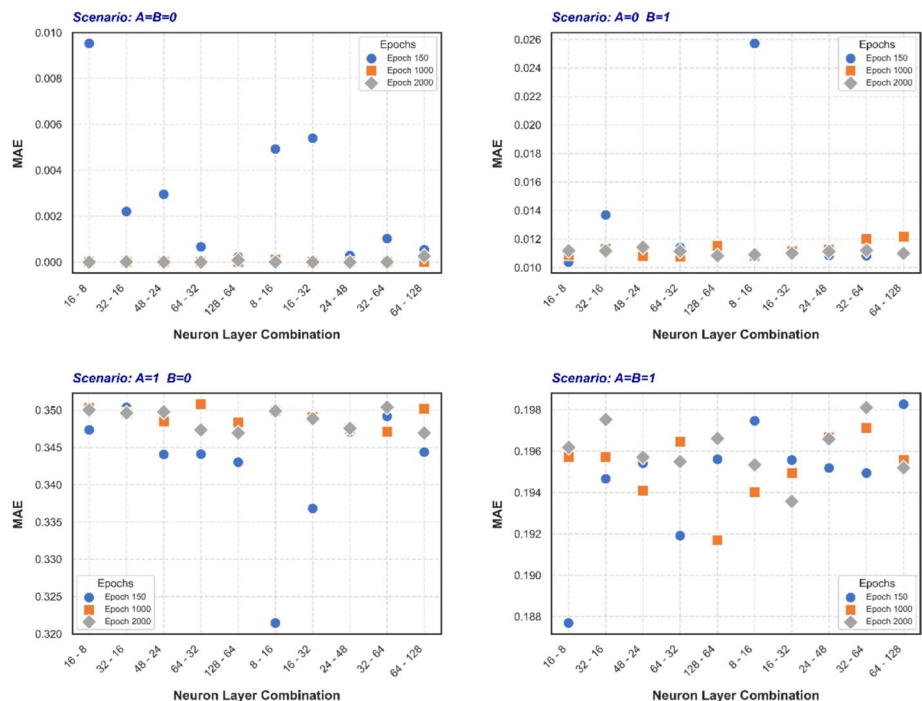


**Fig. 4** Performance of FNN Models in Predicting Optimal phi 3 for NOR Gate Operation Across Different Input Scenarios

To achieve optimal performance for the optical NOR gate, we investigated the effectiveness of various FNN architectures in predicting the ideal phi parameter. We trained 30 different FNN models, each with a unique combination of neuron layers and training epochs, as depicted in Fig. 3. For further information and detailed results, please refer to the supplementary file "*model\_results\_FNN.csv*". By analyzing the trends in the figure, we can identify the FNN architecture and training epoch that yields the lowest MAE for each input scenario. This analysis enables us to select the best-performing model for optimizing the NOR gate under different operating conditions. Similarly, Fig. 4 illustrates the same analysis conducted for the phi 3 parameter, allowing us to determine the optimal FNN architecture and training epochs for its prediction.

### 3.7.5 Visualizing phi 2 and phi 3 optimization with heatmaps

To optimize phi 2 and phi 3 parameters, a comprehensive analysis of various FNN architectures was conducted. Figure 5 presents a heatmap visualizing the performance of these FNN architectures in predicting the phi 2 parameter. Similarly, Fig. 6 provides a heatmap illustrating the effectiveness of different architectures in predicting optimal phi 3 values across various input scenarios. Heatmaps offer a significant advantage in this context as they provide an intuitive and concise representation of complex data, allowing for easy identification of performance trends across multiple variables, such as neuron layer combinations and input scenarios.

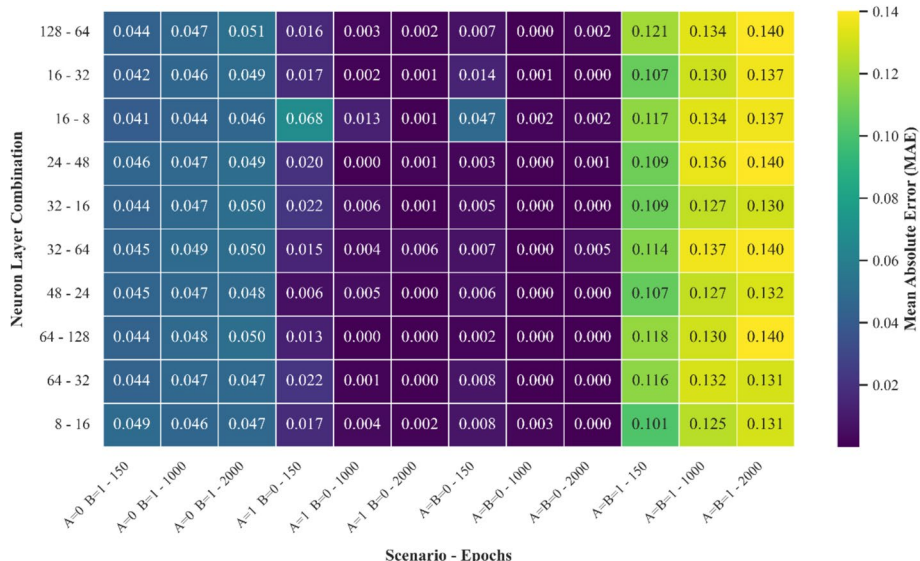


**Fig. 5** Visualizing Phi 2 Optimization with FNN Architectures using Heatmaps

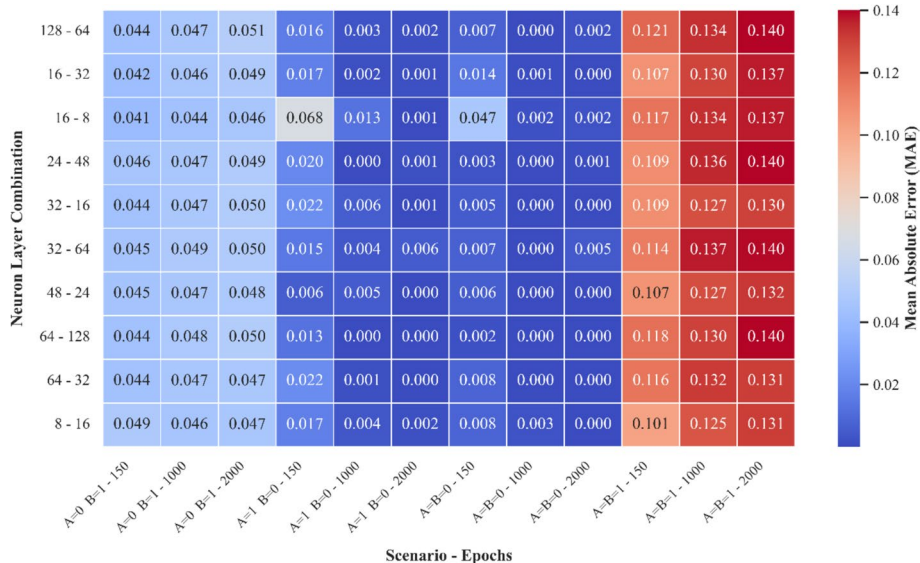


**Fig. 6** Visualizing Phi 3 Optimization with FNN Architectures using Heatmaps

### 3.7.6 Summary of best FNN architectures for predicting phi 2 and phi 3

Table 4 showcases the effectiveness of different neural network architectures, focusing on variations in neuron counts across hidden layers and training epochs. Each scenario represents a distinct configuration aimed at optimizing the prediction of phi 2 and phi 3 in

optical gate design. All models have a base architecture with 1 neuron in the input layer and 4 neurons in the output layer.

The architectures vary significantly between scenarios, reflecting the adaptability of the models to different input dynamics. For example, the configuration for the scenario employs 64 neurons in the first hidden layer and 32 in the second layer, trained over 2000 epochs for Phi 2. In contrast, a simpler configuration of 16 neurons in the first hidden layer and 8 neurons in the second layer is used for Phi 3 under the same scenario. This highlights the importance of tailoring neural network architectures to specific prediction tasks, as the choice of neurons and epochs can greatly influence model performance (See Table 4).

Figure 7 illustrates the neural network architectures employed for predicting Phi 2 and Phi 3 across various input scenarios ( $A=B=0$ ,  $A=1, B=0$ ,  $A=0, B=1$ ,  $A=B=1$ ). Each architecture is visually represented, depicting the specific number of neurons in each layer (input, hidden layers 1 and 2, and output). Crucially, this visualization demonstrates how the architecture varies significantly across different input scenarios. For example, the architecture optimized for predicting Phi 2 when  $A=B=0$  might have more neurons in its hidden layers than the architecture optimized for predicting Phi 3 under the same input conditions or a different number of neurons than the architecture designed for predicting Phi 2 when  $A=1, B=0$ . This difference in the number of neurons, and potentially their arrangement across the layers, reflects the differing complexities of the underlying relationships between the input parameters and the output values (Phi 2 and Phi 3) for each scenario. The figure directly translates the numerical data from Table 4 into a visual format, highlighting the tailored architectures for each specific input condition and showing how these choices affect performance as measured by MAE in the Table 4 layer, reflecting the specific input conditions.

### 3.7.7 Evaluation of best FNN models for optimizing phi 2 and phi 3

Table 5 summarizes the mean value  $\pm$  standard deviation for both MAE and RMSE metrics, calculated over 5 trials. These metrics correspond to the neural network architectures listed in Table 4, highlighting the prediction performance of each architecture for Phi 2 and Phi 3 under different scenarios.

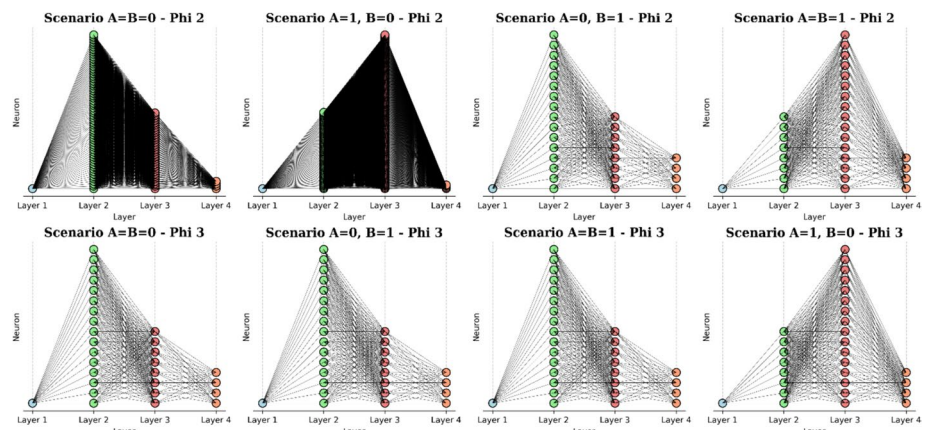


**Fig. 7** Optimized FNN Architectures for Predicting Phi 2 and Phi 3 under Different Input Scenarios

**Table 5** Performance Metrics Based on Optimal Configurations, MAE and RMSE $\pm$  Standard Deviation

Scenario	Phi 2		Phi 3	
	MAE (mean $\pm$ std)	RMSE (mean $\pm$ std)	MAE (mean $\pm$ std)	RMSE (mean $\pm$ std)
A=B=0	0.0106 $\pm$ 0.0110	0.0122 $\pm$ 0.0109	0.0019 $\pm$ 0.0000	0.0019 $\pm$ 0.0000
A=1, B=0	0.0377 $\pm$ 0.0226	0.0461 $\pm$ 0.0291	0.0280 $\pm$ 0.0153	0.0365 $\pm$ 0.0223
A=0, B=1	0.0157 $\pm$ 0.0154	0.0165 $\pm$ 0.0152	0.4542 $\pm$ 0.1553	0.5121 $\pm$ 0.1510
A=B=1	0.0206 $\pm$ 0.0107	0.0223 $\pm$ 0.0113	0.0725 $\pm$ 0.0385	0.0814 $\pm$ 0.0427

The MAE and RMSE values reflect the models' ability to generalize from training data to unseen data, with lower values indicating better predictive accuracy. For example, in the scenario A=B=0 for Phi 2, the model achieved a strong MAE of  $0.0106 \pm 0.0110$  and an RMSE of  $0.0122 \pm 0.0109$ , demonstrating its robustness in this condition. On the other hand, the scenario A=1, B=0 for Phi 3 shows significantly higher error metrics with an MAE of  $0.4542 \pm 0.1553$  and an RMSE of  $0.5121 \pm 0.1510$ , illustrating the increased difficulty of this particular prediction task (See Table 5).

Overall, the values in Table 5 emphasize the strong correlation between the architectural choices made in Table 4 and the resulting predictive performance of the models. This underscores the importance of selecting appropriate neural network structures to achieve optimal results in the design of optical logic gates.

## 4 Results

### 4.1 Realization of optical NAND and NOR gates

Simulations were performed for different input states to validate the proposed structure's functionality as a NAND and NOR gate. Rsoft CAD software was used to simulate the structure and optical power distribution diagram in the structure and calculate the output power. This software is suitable for simulating photonic crystal structures.

#### 4.1.1 Realization of optical NAND gate

Simulations were performed for different input states to validate the proposed structure's functionality as a NAND and NOR gate.

Considering the previously mentioned input phase differences, four input states were simulated to create an optical NAND gate. The input phase difference for A relative to the bias input was set at -45 degrees and for B at +45 degrees. Figure 8 shows the simulation results for all the input states.

Figure 9 illustrates the normalized output power graphs calculated for the four different input states. The results indicate that in three states, where at least one input is "0", the output power is high, and only when both inputs are "1", the output power is very low.

The graphs in Fig. 10 demonstrate that this structure can function as a NAND gate. When both inputs are "1" (i.e., both input sources A and B are on), the output is very low, which can be considered as a logical 0. In other states, the output is high, equivalent to a

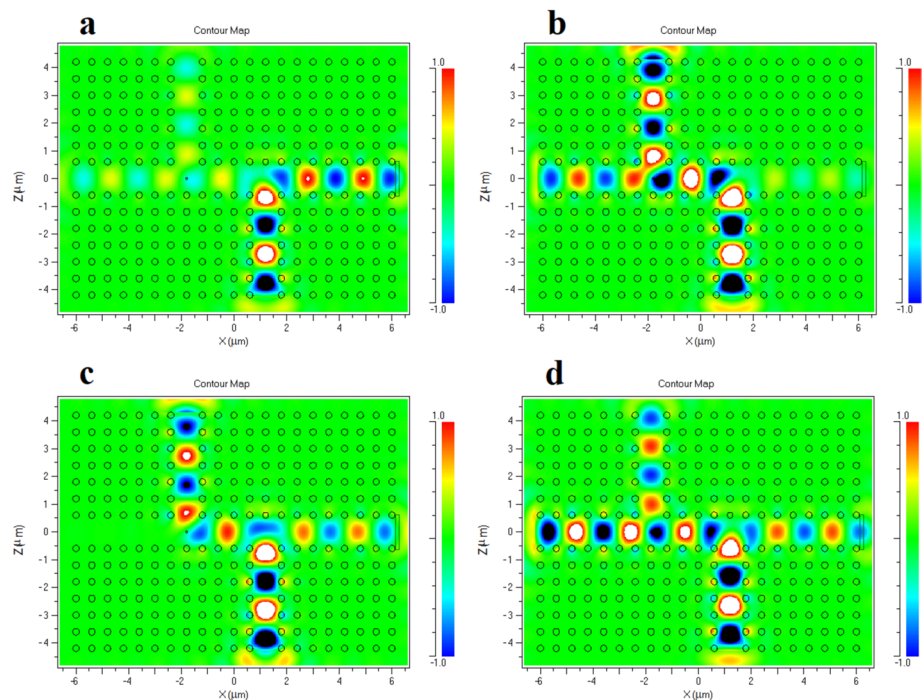


**Fig. 8** Optical Power Distribution for the Proposed Structure as a NAND Gate. **a**  $A=B=0$ , **b**  $A=B=1$ , **c**  $A=0, B=1$  and **d**  $A=1, B=0$

logical “1”, aligning with the behavior of a NAND gate. The numerical values of the output power for different states of the designed NAND gate are provided in Table 6.

#### 4.1.2 Realization of optical NOR gate

To use the proposed structure as an optical NOR gate, the input phase difference for A is set in-phase with the bias input and for B at +10 degrees. The optical power distribution for different input states is shown in Fig. 10. As illustrated, the output is high only when both inputs are “0”, and low in other states, which matches the behavior of a NOR gate.

The normalized output power for the designed optical NOR gate is shown in Fig. 11. Figure 10 shows that the output when both inputs are “0”, has a normalized power of 0.76, which can be considered a logical “1”. The output is very low in other states, corresponding to a logical “0”.

Table 6 shows the values of the output parameters for the proposed NAND and NOR gate, including normalized output power, response time, contrast ratio, and bit rate. The response time here is the time required for the output to reach a stable state. Also, the bit rate parameter has been calculated according to the response time parameter, considering that the drop time after the input signal is cut off is almost equal to the response time. The bit rate parameter is also calculated according to the relation  $BR = 10 \times \log(\frac{P_{1,min}}{P_{0,max}})$ . In this equation, the lowest value is considered for “1”, and the highest value is considered for “0”.

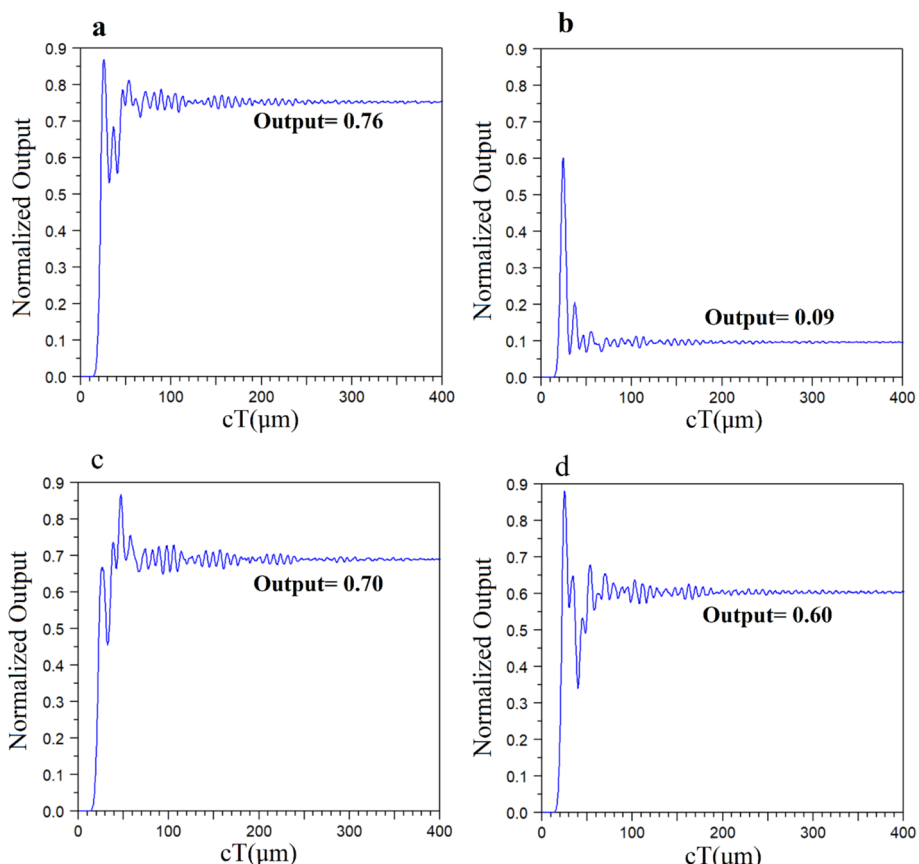


**Fig. 9** Normalized Output Power for the Proposed Structure as a NAND Gate. **a**  $A = B = 0$ , **b**  $A = B = 1$ , **c**  $A = 0, B = 1$  and **d**  $A = 1, B = 0$

#### 4.2 Comparison with related work

In this section, we compare the performance and design of our proposed all-optical NAND and NOR logic gates with existing work in the field. Table 7 presents a detailed comparison.

As seen in Table 7, the proposed structure has a smaller size, which is one of the advantages of this structure. It also has a reasonable bit rate. In reference (Shaik and Rangaswamy 2018b), the bit rate value is significant, but the size of the structure is larger, and its contrast ratio is lower than the proposed structure.

Our work differentiates itself by utilizing a machine learning-based optimization method for adjusting key design parameters such as rod radius and phase. This approach leads to a more efficient and compact design compared to previous works that relied on manual parameter tuning through FDTD simulations. Specifically:

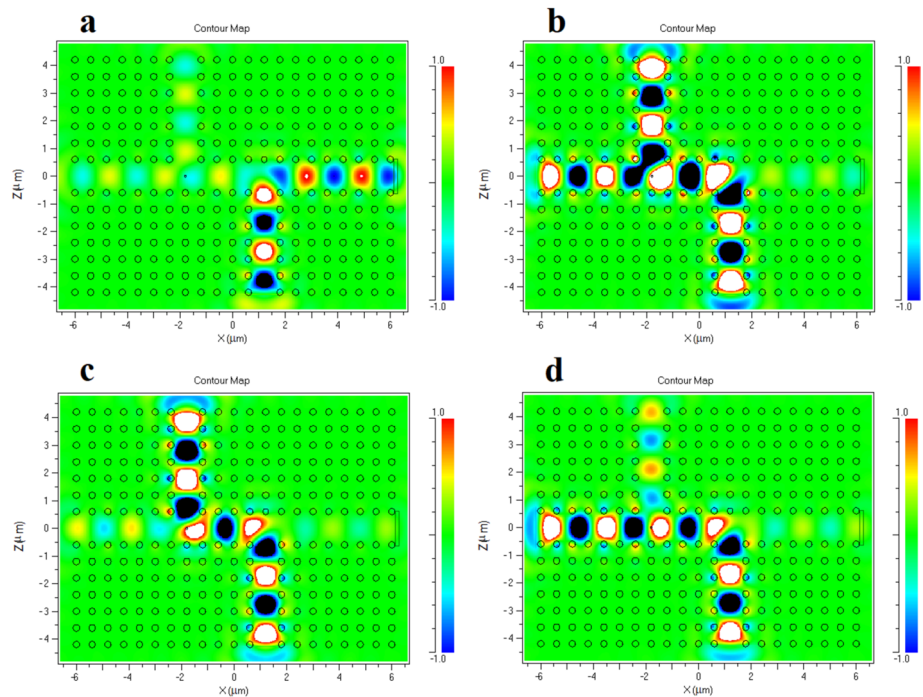


**Fig. 10** Optical Power Distribution for the Proposed Structure as a NOR Gate. **a**  $A=B=0$ , **b**  $A=B=1$ , **c**  $A=0, B=1$  and **d**  $A=1, B=0$

**Table 6** Output Parameters for the Optical NAND and NOR Gate

	Input state	Normalized output power	Response time	Contrast ratio	Bit rate
NAND gate	$A=B=0$	0.76	0.16ps	8.2 dB	2.5 Tb/s
	$A=0, B=1$	0.70	0.2ps		
	$A=1, B=0$	0.60	0.2ps		
	$A=B=1$	0.09	NA		
NOR gate	$A=B=0$	0.76	0.15	8.8 dB	3.3 Tb/s
	$A=0, B=1$	0.08	NA		
	$A=1, B=0$	0.09	NA		
	$A=B=1$	0.10	NA		

- **Optimization method:** While previous works manually adjusted parameters, we employed an AdaBoost Regressor and a FNN to optimize the design. This resulted in a more systematic and faster process of finding optimal configurations.
- **Input phase control:** Our design uses input phase control to switch between NAND and NOR operations within a single structure, enhancing flexibility and reducing the need for separate structures for each logic function.

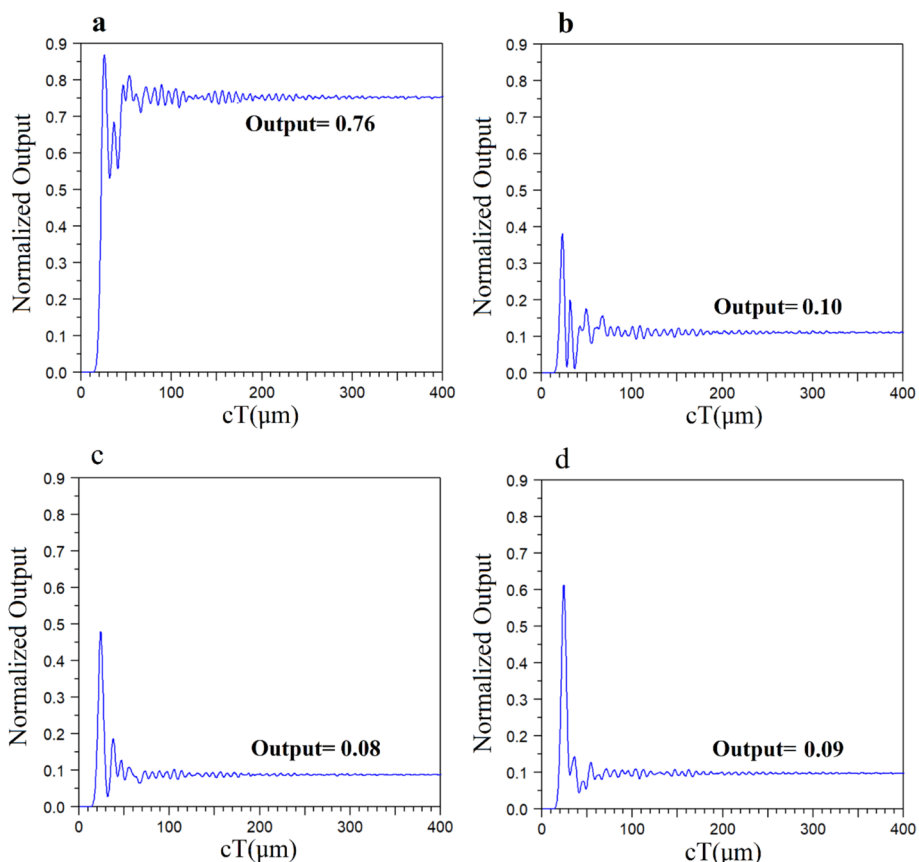


**Fig. 11** Normalized Output Power for the Proposed Structure as a NOR Gate. **a**  $A=B=0$ , **b**  $A=B=1$ , **c**  $A=0, B=1$  and **d**  $A=1, B=0$

**Table 7** Comparison of key features between the current work and previous studies on photonic crystal-based optical logic gates

References	Footprint ( $\mu\text{m}^2$ )	Contrast Ratio (dB)		Response Time (ps)		Bit Rate (Tb/s)	
		NAND	NOR	NAND	NOR	NAND	NOR
Mamnoon-Sofiani and Javahernia (2023)	988	8.7	9.5	2.5	2.5	0.2	0.2
Shaik and Rangaswamy (2018a)	280	10.5	8.6	0.15	0.15	3.3	3.3
Rani et al. (2017)	218	12.48	—	2.16	—	0.23	—
Shaik and Rangaswamy (2018b)	309	5.81	4.02	0.124	0.133	4.03	3.75
This work	189	8.2	8.8	0.35	0.15	2.5	3.33

## 5 Discussion

This work presents a novel approach to optimizing NAND and NOR gates using a two-dimensional photonic crystal structure composed of dielectric rods in an air substrate. Our research leverages advanced machine learning techniques, specifically the AdaBoost Regressor and FNN models, to enhance the performance of these gates by optimizing critical parameters such as the rod radius and phi. This method significantly improves the overall efficiency of optical logic gates compared to traditional optimization techniques.

### 5.1 Comparative performance analysis

In the field of optical logic gate design, various optimization methods have been explored to enhance the efficiency, scalability, and performance of photonic crystal structures. Table 8 presents a comparison between our proposed optimization method and several existing approaches used in similar studies.

This comparison emphasizes several key points:

- **Unique optimization approach:** Our work focuses on optimizing the rod radius and phase (phi) in a two-dimensional photonic crystal using a combination of AdaBoost Regressor and FNN. This dual approach provides precise tuning of structural parameters, which contrasts sharply with the numerical methods used in other quantum gate designs like in Gerasimov et al. (2023), where the optimization focuses solely on solving the effective Hamiltonian of cold atom traps for Controlled-Z logic gates. In contrast, our method automates parameter tuning, making it more practical and efficient for designing multiple all-optical logic gates, including NAND and NOR, which are crucial for integrated photonic circuits.
- **Broader parameter optimization:** Compared to Parandin et al. 2023b, which utilizes ANN for optimizing the rod radius in a photonic crystal-based AND gate, our method is more versatile. By extending the optimization to both the rod radius and phase, our approach supports a broader range of logic gates, such as NAND and NOR. While (Parandin et al. 2023b) demonstrates the applicability of ANNs in optimizing structural parameters, their approach is limited to a single gate (AND), and lacks generalization for other logic gates. Furthermore, our optimization strategy encompasses multiple parameters and improves scalability, whereas their study does not provide a clear optimization formula for parameter tuning.
- **Evolutionary algorithms vs. machine learning:** Optimization techniques like particle swarm optimization (PSO) and the nondominated sorting genetic algorithm II (NSGA-II), used in Mousavi et al. (2024) and (Dan et al. 2022), have proven effective for global optimization of metasurfaces and coding metamaterials, respectively. However, these evolutionary algorithms often come with high computational costs. PSO, as used by Mousavi et al. (2024) to optimize metasurface unit cells, and NSGA-II, applied by Dan et al. (2022) for coding metamaterial distributions, provide robust solutions but require significant computational time and resources. Our approach using AdaBoost and FNN balances computational efficiency and accuracy, offering a faster optimization process (under 30 s), which makes it ideal for real-time applications in photonic circuits.
- **Automated parameter tuning:** A key advantage of our method is the automation of parameter tuning, which significantly reduces the time and errors associated with

**Table 8** Comparison of Optimization Methods for Photonic Crystal All-Optical Logic Gates

Feature	Current work	Gerasimov et al. 2023)	Parandin et al. 2023b)	Mousavi et al. 2024)	Dan et al. 2022)
Structure	2D Photonic Crystal, square lattice, dielectric rods in air	Cold atoms in optical microtraps	2D Photonic Crystal, grid of rods	Meta surface unit cell based on coherent perfect absorber	Metal-Dielectric-Metal (MDM) coding metamaterials
Logic gates	NAND, NOR	Controlled-Z (CZ) logic gate	AND gate	NOT, AND OR, NAND, NOR, XOR, XNOR	All-type (AND, OR, NOT, NAND, NOR, XOR, XNOR)
Optimization method	AdaBoost Regressor, FNN for parameter optimization (rod radius, phi)	Numerical solution of effective Hamiltonian	ANN (MLP) for optimizing rod radius	Particle Swarm Optimization (PSO) for optimizing meta surface unit cell dimensions	Non-dominated Sorting Genetic Algorithm II (NSGA-II) for optimizing coding metamaterial distributions
Rod radius and phase optimization	AdaBoost Regressor and FNN used for precise tuning of rod radius and phi	Not applicable	ANN used for rod radius optimization	PSO used for optimizing radius of circular elements	NSGA-II used for coding metamaterial distributions

manual approaches commonly used in traditional optimization techniques. By employing machine learning models like AdaBoost and FNN, we are able to explore a wider design space and rapidly identify optimal solutions. This automation makes it possible to precisely tune critical parameters such as lattice constant, rod radius, and so on. Evidently, the success of this approach depends on the performance of the chosen machine learning model on the specific dataset. For example, achieving a high level of accuracy, with a MAE close to 0.1, ensures that the optimal parameters can be reliably determined. This flexibility distinguishes our method from approaches in Gerasimov et al. (2023); Mousavi et al. 2024), and (Dan et al. 2022), which depend on evolutionary or manual tuning, making our approach both faster and more robust.

In summary, While the methods in Mousavi et al. (2024) and (Dan et al. 2022) showcase the robustness of evolutionary algorithms for global optimization, the ML approach in our work offers a more flexible, efficient, and scalable solution. By focusing on multiple key parameters and achieving fast, real-time optimization, our work stands out as a practical alternative for the rapid development of high-performance photonic crystal logic gates. However, one of the challenges is that finding a ML model with acceptable accuracy can be challenging in complex or noisy datasets.

## 5.2 Implications and future work

The integration of AdaBoost Regressor and FNN into the optimization of 2D photonic crystal-based logic gates has significant implications for the future of optical computing. This methodology provides a robust and adaptable solution for designing more efficient and compact optical logic circuits. The improved accuracy and performance demonstrated in this study suggest that machine learning techniques can play a crucial role in the next generation of optical computing systems.

Future work will focus on further refining the models by exploring other machine learning algorithms and expanding the scope of optimization to more complex photonic structures and integrated optical circuits. Additionally, we aim to investigate the scalability of our approach for larger photonic networks and its application in areas such as optical data processing and high-speed communication systems.

## 6 Conclusion

In this study, we presented a novel approach to optimize the performance of optical NAND and NOR gates using a two-dimensional photonic crystal structure with dielectric rods. By employing advanced machine learning techniques, specifically the AdaBoost Regressor and FNN models, we successfully identified the optimal parameters to enhance gate performance. This research marks optimizing the phi parameter and rod radius using these models, leading to significant improvements in the gate's output power characteristics. Furthermore, we evaluated 30 different architectures to determine the best FNN model for each scenario. Our findings demonstrate that integrating machine learning methodologies into the design process of optical logic gates can significantly advance the performance and reliability of integrated optical circuits.

**Author's contribution** PK designed and performed simulations. AM and FP analyzed data and wrote the manuscript. FP supervised, edited, and prepared the final draft of the manuscript. All authors read and approved the final manuscript.

**Funding** This article has no funding.

**Data availability** The datasets used in this study are available from the corresponding author upon reasonable request. No datasets were generated or analysed during the current study.

## Declarations

**Conflict of interest** The authors declare no competing interests.

## References

- Abadi, M., Barham, P., Chen, J., Chen, Z., Davis, A., Dean, J., et al.: {TensorFlow}: a system for {Large-Scale} machine learning. In: 12th USENIX Symposium on Operating Systems Design and Implementation (OSDI 16) (pp. 265–283) (2016)
- Agarap, A.F.: Deep learning using rectified linear units (relu). arXiv preprint [arXiv:1803.08375](https://arxiv.org/abs/1803.08375) (2018)
- Askarian, A.: Design and analysis of all optical  $2 \times 4$  decoder based on kerr effect and beams interference procedure. Opt. Quant. Electron. **53**, 291 (2021)
- Askarian, A., Parandin, F.: Performance analysis of all-optical 1-bit comparator using 2D-PhC nonlinear ring resonators based on threshold switching method. Electromagnetics **43**(8), 562–576 (2023)
- Dan, Y., Fan, Z., Sun, X., Zhang, T., Xu, K.: All-type optical logic gates using plasmonic coding metamaterials and multi-objective optimization. Opt. Exp. **30**(7), 11633–11646 (2022)
- Gerasimov, L.V., Kupriyanov, D.V., Straupe, S.S.: Optimization of entangling logic gates based on the rydberg blockade effect. J. Exp. Theor. Phys. **137**(2), 157–162 (2023)
- Geron, A.: Hands-on machine learning with scikit-learn, keras, and tensorflow: concepts, tools, and techniques to build intelligent systems (2nd. ed.). O'Reilly Media, Inc., (2019)
- Ghadrdan, M., Mansouri-Birjandi, M.A.: Concurrent implementation of all-optical half-adder and AND & XOR logic gates based on nonlinear photonic crystal. Opt. Quant. Electron. **45**, 1027–1036 (2013)
- Gupta, M.M., Medhekar, S.: All-optical NOT and AND gates using counter propagating beams in nonlinear Mach-Zehnder interferometer made of photonic crystal waveguides. Optik **127**, 1221–1228 (2016)
- Karkhanehchi, M.M., Parandin, F., Zahedi, A.: Design of an all optical half-adder based on 2D photonic crystals. Photon Netw. Commun. **33**, 159–165 (2017)
- Liu, W., Yang, D., Shen, G., Tian, H., Ji, Y.: Design of ultra compact all-optical XOR, XNOR, NAND and OR gates using photonic crystal multi-mode interference waveguides. Opt. Laser Technol. **50**, 55–64 (2013)
- Lotfi, S., Roshani, S., and Roshani, S.: Design of a miniaturized planar microstrip Wilkinson power divider with harmonic cancellation. Turk. J. Electrical Eng. Comput. Sci. **28**, 6. Article 3 (2020)
- Mamnoon-Sofiani, H., Javahernia, S.: All optical NAND/NOR and majority gates using nonlinear photonic crystal ring resonator. J. Opt. Commun. **44**(1), 293–302 (2023)
- Mohammadi, A., Parandin, F., Ghahramani, H.: Neural network-driven optimization of photonic crystal-based all-optical NOT gate design. In: 2024 Third international conference on distributed computing and high performance computing (DCHPC) (pp. 1–6). IEEE (2024)
- Moradi, R.: All optical half subtractor using photonic crystal based nonlinear ring resonators. Opt. Quant. Electron. **51**, 119 (2019)
- Mousavi, S., Mansouri-Birjandi, M.A., Rakhshani, M.R., Rezaei, M.: All-optical logic gates based on optimized coherent perfect absorber and fuzzy inference system. Opt. Contin. **3**(7), 1208–1223 (2024)
- Mukherjee, B., Kumar, V.D., Gupta, M.: A novel hemispherical dielectric resonator antenna on an electromagnetic band gap substrate for broadband and high gain systems. Int. J. Electronics Commun. (AEU) **68**, 1185–1190 (2014)
- Neisy, M., Soroosh, M., Ansari-Asl, K.: All optical half adder based on photonic crystal resonant cavities **35**(2), 245–250 (2018)
- Ojha, V.K., Abraham, A., Snášel, V.: Metaheuristic design of feedforward neural networks: a review of two decades of research. Eng. Appl. Artif. Intell. **60**, 97–116 (2017)
- Olyaei, S.: Ultra-fast and compact all-optical encoder based on photonic crystal nano-resonator without using nonlinear materials. Phot. Lett. Pol. **11**(1), 10–12 (2019)

- Olyaei, S., Seifouri, M., Mohebzadeh-Bahabady, A., et al.: Realization of all-optical NOT and XOR logic gates based on interference effect with high contrast ratio and ultra-compacted size. *Opt. Quant. Electron.* **50**, 385 (2018)
- Parandin, F.: Realization of ultra-compact all-optical universal NOR gate on photonic crystal platform. *J. Electrical Comput. Eng. Innov.* **9**(1), 1–8 (2021)
- Parandin, F., Bagheri, N.: Design of a  $2 \times 1$  multiplexer with a ring resonator based on 2D photonic crystals. *Res. Opt.* **11**, 100375 (2023)
- Parandin, F., Malmir, M.R.: Low delay time all optical NAND, XNOR and OR logic gates based on 2D photonic crystal structure. *J. Electrical Comput. Eng. Innov.* **8**(1), 1–8 (2020)
- Parandin, F., Mohamadi, A.: Design and optimization of a photonic crystal-based all-optical XOR gate using machine learning. *Majlesi J. Electrical Eng.* **18**(1), 1–9 (2024)
- Parandin, F., Sheykhanian, A.: Designing a circuit for high-speed optical logic half subtractor, international. *J. Circuits Syst. Signal Process.* **16**, 887–891 (2022)
- Parandin, F., Heidari, F., Aslinezhad, M., et al.: Design of 2D photonic crystal biosensor to detect blood components. *Opt. Quant. Electron.* **54**, 618 (2022)
- Parandin, F., Yahya, S.I., Rezaeenia, M., Askarian, A., Roshani, S., Roshani, S., et al.: A neural networks approach for designing compact all-optical photonic crystal based AND logic gate. *J. Opt. Commun.* (2023a). <https://doi.org/10.1515/joc-2023-0328>
- Parandin, F., Yahya, S.I., Rezaeenia, M., Askarian, A., Roshani, S., Roshani, S., Rezaee, S.: A neural networks approach for designing compact all-optical photonic crystal based AND logic gate. *J. Opt. Commun.* (2023b). <https://doi.org/10.1515/joc-2023-0328>
- Parandin, F., Olyaei, S., Heidari, F., Soroosh, M., Farmani, A., Saghaei, H., et al.: Recent advances in all-optical half-subtractor and full-subtractor based on photonic crystal platforms. *J. Opt. Commun.* (2024a). <https://doi.org/10.1515/joc-2023-0314>
- Parandin, F., Sheykhanian, A., Askarian, A.: A novel design of an all-optical D flip-flop based on 2D photonic crystals. *Microw. Opt. Technol. Lett.* **66**(1), 1–8 (2024b)
- Parandin, F., Mohammadi, A.: Enhancing the performance of photonic crystal AND gates with machine learning optimization. In: 2024 Third international conference on distributed computing and high-performance computing (DCHPC) (pp. 1–7). IEEE (2024c)
- Pedregosa, F., Varoquaux, G., Gramfort, A., Michel, V., Thirion, B., Grisel, O. et al.: Scikit-learn: machine learning in Python. *J. Mach. Learn. Res.* **12**, 2825–2830 (2011)
- Rani, P., Fatima, S., Kalra, Y., Sinha, R.K.: Realization of all optical logic gates using universal NAND gates on photonic crystal platform. *Superlattices Microstruct.* **109**, 619–625 (2017)
- Rani, P., Yogita, K., Sinha, R.K.: Design of all optical logic gates in photonic crystal waveguides. *Opt. Int. J. Light Electron Opt.* **126**, 950–955 (2015)
- Rosenblatt, F.: The perceptron: a probabilistic model for information storage and organization in the brain. *Psychol. Rev.* **65**(6), 386 (1958)
- Roshani, S., Yahya, S.I., Roshani, S., Rostami, M.: Design and fabrication of a compact branch-line coupler using resonators with wide harmonics suppression band. *Electronics* **11**(5), 793 (2022)
- Rumelhart, D.E., Hinton, G.E., Williams, R.J.: Learning representations by back-propagating errors. *Nature* **323**(6088), 533–536 (1986)
- Saghaei, H.: Supercontinuum source for dense wavelength division multiplexing in square photonic crystal fiber via fluidic infiltration approach. *Radioengineering* **26**(1), 16–22 (2017)
- Schapire, R.E.: Explaining adaboost. In: Empirical inference: festschrift in honor of Vladimir N. Vapnik (pp. 37–52). Berlin, Heidelberg: Springer Berlin Heidelberg (2013)
- Seraj, Z., Soroosh, M., Alaei-Sheini, N.: Ultra-compact ultra-fast 1-bit comparator based on a two-dimensional nonlinear photonic crystal structure. *Appl. Opt.* **59**, 811–816 (2020)
- Shaik, E.H., Rangaswamy, N.: Single photonic crystal structure for realization of NAND and NOR logic functions by cascading basic gates. *J. Comput. Electron.* **17**, 337–348 (2018a)
- Shaik, E.H., Rangaswamy, N.: Realization of all-optical NAND and NOR logic functions with photonic crystal based NOT, OR and AND gates using De Morgan's theorem. *J. Opt.* **47**, 8–21 (2018b)
- Strong, A.I.: Applications of artificial intelligence and associated technologies. *Science [ETEBMS-2016]*, **5**(6) (2016)
- Swarnakar, S., Kumar, S., Sharma, S.: All-optical half-adder circuit based on beam interference principle of photonic crystal. *J. Opt. Commun.* **39**(1), 13–17 (2018)
- Swarnakar, S., Kumar, S., Sharma, S.: Design of all-optical half-subtractor circuit device using 2-D principle of photonic crystal waveguides. *J. Opt. Commun.* **40**(3), 195–203 (2019)
- Wang, G., Wang, J., Li, S.Y., Zhang, J.W., Wamg, C.W.: One-dimensional alumina photonic crystals with a narrow band gap and their applications to high-sensitivity concentration sensor and photoluminescence enhancement. *Superlattices Microstruct.* **86**, 546–551 (2015)

Wei, W., Lü, W., Han, Y., Zhang, C., Chen, D.: A novel recessed-source negative capacitance gate-all-around tunneling field effect transistor for low-power applications. *Microelectron. J.* **145**, 106126 (2024)

**Publisher's Note** Springer Nature remains neutral with regard to jurisdictional claims in published maps and institutional affiliations.

Springer Nature or its licensor (e.g. a society or other partner) holds exclusive rights to this article under a publishing agreement with the author(s) or other rightsholder(s); author self-archiving of the accepted manuscript version of this article is solely governed by the terms of such publishing agreement and applicable law.